Adaptive Control System of an Insect Brain during Odor Source Localization

Ryo Minegishi, Yosuke Takahashi, Atsushi Takashima, Daisuke Kurabayashi, and Ryohei Kanzaki

Abstract— To realize an autonomous odor source localization robot, we focused on the adaptability of an insect's brain to compensate for rotational disturbances during odor source searching behavior. We manipulated motor outputs to control the sensory feedback of an insect using a brain-machine hybrid system. This system is composed of an insect's head and a two-wheeled mobile robot. The velocity of the robot is proportional to neural activities descending from an insect brain. We successfully manipulated the behavior of the robot. In disturbance experiments, insects responded to given rotational disturbances by modifying their neural activities to make compensative angular velocity. We assumed this control system of the compensation as an output-error model. We calculated the parameters under different motor gains to reveal it as an adaptive controller. We propose that an insect has its appropriate angular velocity during odor source localization, and performed simulation experiments involving an odor source searching agent and odor distribution environment. We calculated the cost for odor source localization by changing the angular velocity of the agent, and found that it had the minimum value.

I. INTRODUCTION

There is a need for a technology that assists in locating injured persons or dangerous objects (such as toxic gases) in disaster sites. In most cases, scents that are released from them are traced to locate the odor sources. This task is called chemical plume tracing (CPT) and is not easily solved by artificial systems because scents that are distributed as plumes [1], [2], show trajectories that cannot be easily modeled and the odor environment is almost unpredictable. We usually rely on the noses of dogs to solve this task. However, it takes a long time to train dogs and there is an ethical issue regarding the use of animals in dangerous places. There is therefore the need for an autonomous robot that can trace an odor source. To date, however, there has been no success in the development of a practical design.

On the other hand, various animals have the ability to locate odor sources, and their strategies of localization have been studied [3]. Insects are among such animals [4], [5], [6], [7], [8], [9]. Even though their brain size is comparatively small,

they can adapt to localize an odor source to ensure survival in changing environmental conditions [10].

In this study, based on biological experiments we performed, we evaluated the important behavioral parameters in an insect's effective CPT. To control the behavioral parameter, we used a brain-machine hybrid system which we developed [11], [12]. The brain-machine hybrid system is a two-wheeled mobile robot controlled by neural activities relating to steering behavior recorded from an insect's head mounted on the robot. Using this system, we manipulated the motor output of the robot by giving disturbances as angular velocity and translational velocity to control the relationship between a brain and environment. We add arbitrary movement on the robot controlled by the command signals from the brain. Moreover, in simulation experiments, we evaluated a behavioral parameter by calculating the costs for odor source localization.
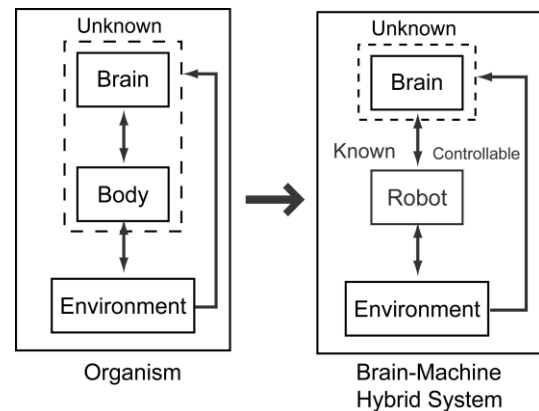

Fig. 1. Composition of a brain-machine hybrid system compared with that of organism. In an organism, the brain and body are inseparable. In the brain-machine hybrid system, we can separate and identify functions of a brain using a robot which is controllable, allowing it to interact with real environments.

II. BRAIN-MACHINE HYBRID SYSTEM

We used a male silkworm moth as an experimental animal. Male silkworm moths orient toward conspecific females by displaying a programmed behavioral pattern upon detection of sex pheromones by their antennae. This behavior consists of straight-line walking, zigzagging turns and looping [13], [14], [15], [16]. Silkworm moths reset and restart this behavior every time they detect female sex pheromones. Because the

relationship between input stimulus and output behavior is clear, it is a suitable CPT model to use in analysis. In addition to their behavioral pattern, they do not fly and their orientation trajectories can be analyzed in a two dimensional surface.

We recorded neural activities related to turn walking and reconstructed the moth's behavior on the robot. We used the activities of neck motor neurons 2nd CNb (2nd cervical nerve b) [11], [12]. 2nd CNbs consist of 5 motor neurons and innervate to neck muscles, which contract during horizontal side-wise head movement. There is a pair of 2nd CNbs, and head swing is caused by the contraction of complementally muscles' regulated by bilateral 2nd CNbs [17]. Based on simultaneous recording of head swing and walking, the angular velocity of the moths' turning walk and angle of head swing were found to be in agreement [17], [18].

Details of the signal recording methods have already been described in previous works [11], [12], [17], [18]. We applied two glass micro-electrodes to suck the cut ends of the right and left 2nd CNb nerves. Recorded raw signals were amplified and filtered through small amplifiers [11], [12] on the robot (e-puck, EPFL), and acquired signals were processed in a micro-computer of the robot for conversion into motor outputs (wheels' rotation).

Neural activities are shown as waveforms such as spines, and we refer to them as spikes, where a spike is a unit of neural activities. To quantify neural activities of the bilateral 2nd CNbs, we set thresholds to count spikes. We set a spike-behavior conversion rule to reconstruct a moth's behavior on a robot [11], [12]. The forward velocity is proportional to the sum of the right and left 2nd CNbs' spiking rates. The angular velocity is proportional to the difference between the right and left 2nd CNbs' spiking rates. A proportional constant was calculated from the average walking speed (26 mm/s) in behavioral experiments and average spiking rate (6.5 spikes/0.1 s) in physiological experiments. The control cycle of the hybrid system is 0.1 second.
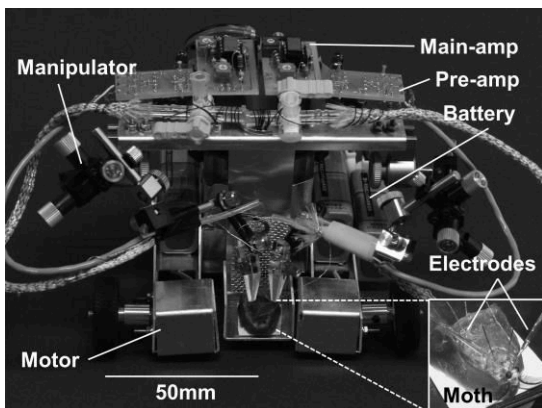

Fig. 2. Picture of a brain-machine hybrid system. Neural signals recorded from an insect using two electrodes are amplified and processed for conversion into motor outputs of the mobile robot. i.e. a moth on the robot with sensors is a living controller of the artificial body.

III. MODELL OF FEEDBACK CONTROL SYSTEM IN INSECT AND THE HYBRID SYSTEM

The hybrid system can use sensory information by using a silkworm moth's sensors including antennae, compound eyes, and other sensory organs. To identify the sensory feedback system in the brain, we assumed a functional block diagram of this hybrid system. We set frameworks of feedback control systems between a silkworm moth's sensors and an artificial body's motor output. Here, we focused on the sensory feedback system including a plant (P, a robot), a controller (C, a brain) and a sensor (S) (Fig. 3). Command signals for the behavioral patterns are generated in the upper region of the brain, and the pattern is then modified in feedback systems in the brain by using sensory feedbacks (Fig. 3). Using the brain-machine hybrid system, we can separate functions of a brain and body by independently giving disturbances in the artificial body to identify the controller of the feedback system.
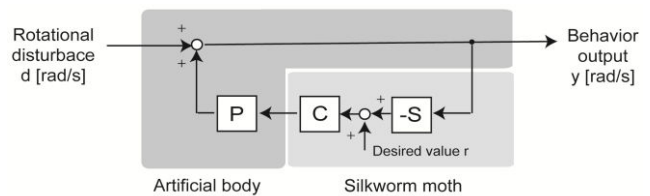

Fig. 3. Feedback control system in the brain-machine hybrid system. Desired value r from the premotor area in a brain is the command signals. A disturbance (in this figure, the rotational angular velocity d) given to a robot (P, plant) is fed back to the brain (C, controller) through sensors (S). If there are any adaptive feedback mechanisms, the disturbance will be cancelled out in behavior outputs (in this figure, y) by changing the neural spike rate.

IV. DISTURBANCE EXPERIMENTS ON AN BRAIN-MACHINE HYBRID SYSTEM

For the first step of the disturbance experiments, we gave the robot forced movement and recorded its neural responses. We rotated the robot with an angular velocity 1.0 rad/s independent of 2nd CNb's spiking rates. The moth on the robot responded to rotational movement (Fig. 4). The right and left 2nd CNbs were excited in response to the counterclockwise and clockwise rotations, respectively. These responses disappeared when the compound eyes were covered by aluminum foil. These results indicate that the responses were caused by visual feedback. Because the moth was set ventral-side up (Fig. 2), each 2nd CNb's excitation followed ipsi-lateral optical flow caused by rotational movement. In general, flying insects keep their body axis constant using directional optical cues [19], [20], [21], [22], [23].

The 2nd CNbs only responded to rotational forced movement which induced an angular velocity. The responses to rotational movement increased as the angular velocity increased (Fig. 5). There was no response in the 2nd CNbs during forced translational movement which induced forward velocity.
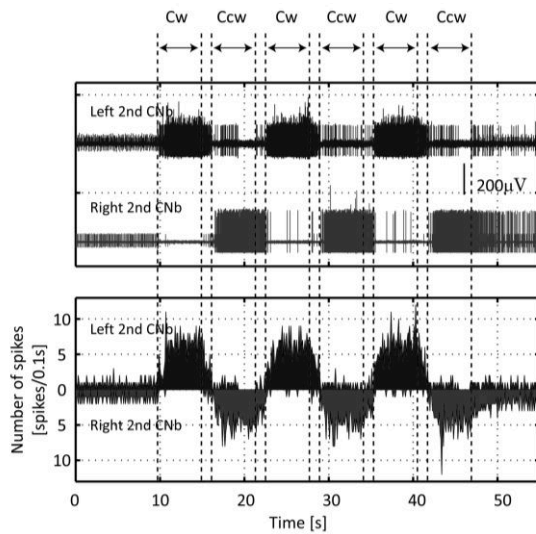
Fig. 4. Typical neural responses of a moth to rotational movement of the robot. Upper graph shows both 2nd CNbs' neural activities responding to forced rotational movement (1.0 rad/s) on a robot. We switched 5 s clockwise and counterclockwise rotations. The lower graph shows histograms of spiking number corresponding to the upper neural activities. The bin width of the histogram is 0.1 s. Cw: clockwise rotation. Ccw: counterclockwise rotation.

Fig. 6. Protocol of disturbance experiments. Disturbances as angular velocity were given to the mobile hybrid system as steps adding to motor outputs. Disturbances were given as 2 pairs of clockwise and counterclockwise rotations with 5 s intervals. To avoid responses caused by learning or adaptation, we introduced disturbances for 4 different durations and shuffled the order.
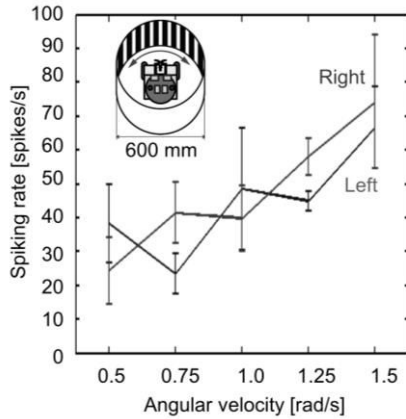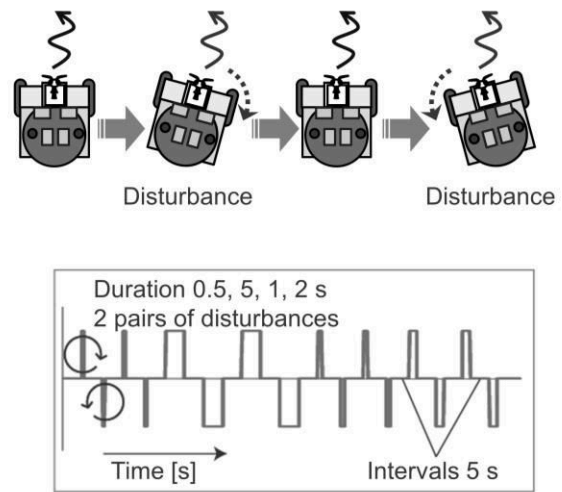

Fig. 5. Response properties of right and left 2nd CNbs to given rotational movement for different angular velocities. In this graph, "Right" and "Left" bars represent right and left 2nd CNb's responses to counterclockwise and clockwise rotations, respectively. The hybrid system was rotated at the center in a cylindrical arena. The diameter of the arena is 600 mm, while its height 526 mm. The inside wall of the arena is patterned with sinusoidal stripes to duplicate a visual condition. The width of a stripe is 47.5 mm. Spiking rates with standard deviations were averaged results of 30 trials from different individuals.

From the response properties of the 2nd CNbs described above, for the next step, we introduced the angular velocity as disturbances to the hybrid system. In this experiment, the hybrid system is mobile using the robot converting steering neural signals acquired from the moth. We investigated the ability of a moth on the hybrid system to cancel disturbances using their own steering command signals. Disturbances were added to the motor outputs of the robot as increments of angular velocity (1.0 rad/s) with direction (clockwise or counterclockwise rotation) for different durations (0.5-5.0 s) and intervals (5 s) (Fig. 6).

With the hybrid system, a moth could cancel out disturbances using compensative neural responses to maintain its body position (Fig. 7). When the clockwise rotation was given, the view from a moth on the robot flew from right to left, and the left 2nd CNb was excited to follow the view. Then, the excitation made the robot turn in a counterclockwise direction to compensate for the given disturbance. This response is the same as that shown in Fig. 4.

Fig. 7 shows the given disturbances as increments with the direction and neural responses converted into angular velocity. The motor output of the hybrid system is the sum of disturbances and neural outputs. The motor output in Fig. 7 shows that neural outputs in directions opposite the angular velocity of the disturbances cancel out the disturbances.

Then, we changed a spike-behavior conversion rule of the hybrid system into an angular velocity double condition and introduced disturbances as in the normal condition (Fig. 6). As we mentioned in section II, we set the angular velocity of the hybrid system proportional to the difference between the right and left 2nd CNbs' spiking rates. A proportional constant was calculated from the average walking speed (26 mm/s) in behavioral experiments and average spiking rate (6.5 spikes/0.1 s) in physiological experiments. We doubled the proportional constant in the angular velocity doubled condition. Even though the conversion rule had changed, the angular velocity disturbances given to the hybrid system were cancelled out by neural responses. This means that the neural function compensative to disturbances works according to the sensory feedback resulting from motor outputs. From this result, we supposed that there is an adaptive feedback system in the controller (moth's brain) of the hybrid system.
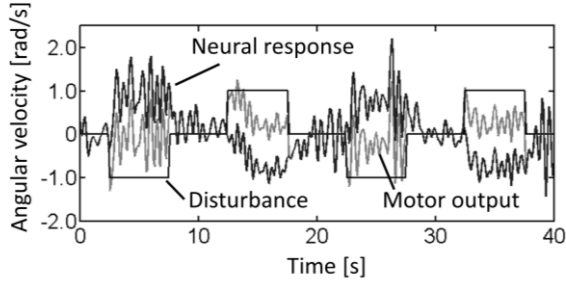
Fig. 7. Typical responses to step disturbances on the hybrid system. This figure shows the time response of the neural response, disturbances and motor output. Neural responses were converted into angular velocity. 1.0 rad/s angular velocities with 5 s duration were given as clockwise and counterclockwise rotational disturbances. The vertical axis indicates the angular velocity. A positive value indicates counterclockwise rotation and a negative value indicates clockwise rotation. The motor output is represented as the sum of disturbances and neural responses.

V. COMPARISON OF PARAMETERS IN TRANSFER FUNCTION (OUTPUT ERROR MODEL)

We applied a system identification method to a supposed feedback control system (Fig. 3) using input and output data (disturbances d [rad/s] and motor outputs y [rad/s]). We estimated the system model parameters using the output error model (OE model). The model is described by the relationship between a function $B(q)$ and a function $F(q)$ as in (1). The function $B(q)$ represents the input characteristics, while the function $F(q)$ represents the output characteristics. This model has three parameters, namely b1, f1 and f2 as in (2). We calculated these parameters using input disturbance data $d(k)$, output behavior data $y(k)$ and white noise $w(k)$.

$$y(k) = \frac{B(q)}{F(q)} d(k) + w(k) \tag{1}$$

$$y(k) = \frac{b_1}{1 + f_1 q^{-1} + f_2 q^{-2}} d(k) + w(k) \tag{2}$$

We calculated the model parameters (b1, f1, f2) based on the neural responses acquired from disturbance experiments in normal angular velocity and doubled angular velocity conditions (Fig. 8). By comparing the parameters of the angular velocity double condition with those of the normal angular velocity condition, we found that there was no significant difference in the parameters between two groups (t-test, $P < 0.05$). This means that the input disturbances were cancelled out by neural responses to keep the behavior outputs constant independent of the spike-behavior conversion rule. In short, a brain can be assumed to be an adaptive controller that keeps the angular velocity constant.
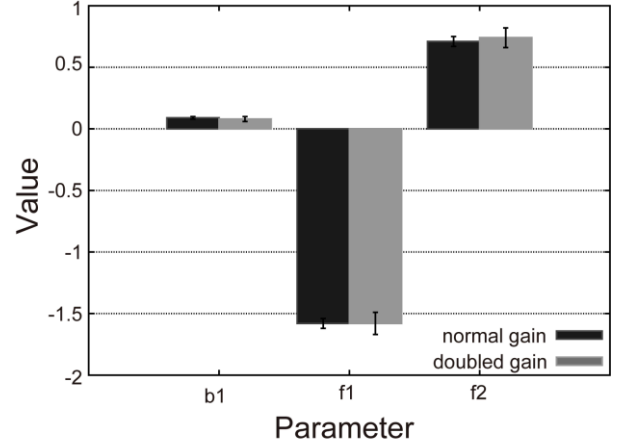

Fig. 8. Parameters in the feedback system model. Parameters in the output error model were calculated using input data and output data acquired from disturbance experiments under different angular velocity conditions (normal gain and double gain). Normal gain and double gain refer to normal angular velocity and angular velocity double conditions. Values shown in bar graphs are the averages of 22 trials in 5 individuals with standard deviations. In each parameter, there was no significant difference between two conditions (t-test, $P < 0.05$).

VI. SIMULATION EXPERIMENTS

From the system identification experiments, we concluded that the moth controlled command neural signals to adapt the different motor gain of the robot. The hybrid system was not just moved by the given spike behavior conversion rule. The system maintained its behavior constant.

A. Simulation Setup

Based on the experimental results regarding the effect of disturbances, we hypothesized that there would be an appropriate angular velocity during odor source localization. We investigated whether the adaptive feedback control system contributed to CPT performance, and carried out simulations to investigate the relationship between the CPT performance and the angular velocity of a moth.

We assumed the behavior model of a moth. A simulated moth agent has two sensors that detect pheromone stimuli. The odor source searching behavior is expressed on a two dimensional coordinate field because silkworm moths cannot fly. They walk to search for an odor source.

We simulated a moth's programmed behavior (straight-line walking, zigzag turns and looping) by setting the average forward velocity, angular velocity and duration acquired from behavioral experiments (Fig. 9) [16]. This programmed behavior resets and restarts every time a moth agent detects a pheromone stimulus.

To investigate whether the CPT performance was related to the angular velocity, we considered the angular velocity during zigzag turns and looping as a variable.
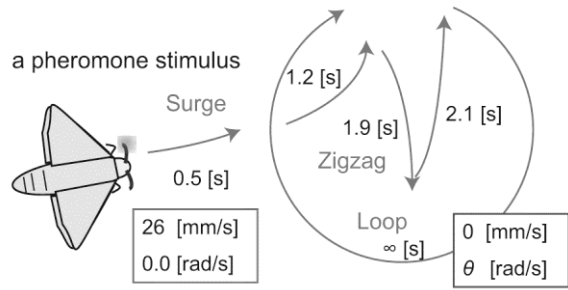
Fig. 9. Behavior model simulated on a moth agent. A simulated moth agent has right and left sensors that detect pheromone stimuli. The programmed behavior of a moth agent consists of a surge (straight-line walking) and following turning behavior (zigzag turns (3 times) and loop). Each behavioral phase has a forward velocity, angular velocity and duration acquired in behavioral experiments. In simulation experiments, angular velocity during zigzag turns and loop behavior is regarded as variable θ.

The sensor that detects the pheromone stimuli is determined by considering the bearing of an agent moth and the wind direction. The direction of the first turn and loop behavior correspond to the side of the antenna which detects the pheromone stimulus (Fig. 9) [24]. We also assumed that a moth agent has a wing flapping effect, which is used to avoid detecting a pheromone stimulus coming from behind. Real moths beat their wings while searching for an odor source. There is therefore an air pocket behind the moth, and moths without wings tend to require more time to localize an odor source than those with wings that are intact [15].

We assumed the pheromone field model which is described as an odor detecting probability density distribution [25]. An odor source was set upwind from the agent's starting point. Considering the upwind direction, the distribution pattern is asymmetric. The distance from the starting point to the target is 512 mm, and the time limit for odor source localization is 720 s.

Using the moth behavior modeled agent and the odor distribution modeled field, we simulated the odor source searching behavior using the variable angular velocity of an agent. We varied the angular velocity of an agent from 0.1 rad/s to 6.3 rad/s for every 0.1 rad/s. We repeated orientation experiments in this simulation and acquired 100 sets of data averaging 100 trials.

B. Evaluation of Performance in Odor Source Localization by Orientation Cost

Based on results acquired in the simulation experiments, we evaluated the CPT performance by calculating the odor source localization cost defined as (3).

$$Cost(\theta) = \log_{10} \frac{T(\theta) \times L(\theta)}{K(\theta)^2} \qquad (3)$$

This cost function is composed of evaluation indices (T, K, L) of the first order lag system. The success rate of odor source localization gradually increases as moth agents arrive at the pheromone source in simulation experiments (Fig. 10). $K(\theta)$ means the rate of success, $L(\theta)$ means the minimum localization time, and $T(\theta)$ means the variance of the localization time. Using these indices, we evaluated the cost for each angular velocity.

If the angular velocity is large, the odor source localization behavior of a moth agent is very uncertain. The agent tends to turn, and the recovery rate required to detect the pheromone stimulus increases. Both K and L become large. If the angular velocity is small, the behavior of an agent is similar to an all-or-nothing approach. Once the agent misses the pheromone stimulus, it gets lost because of the low angular velocity. L becomes small, but T becomes large.
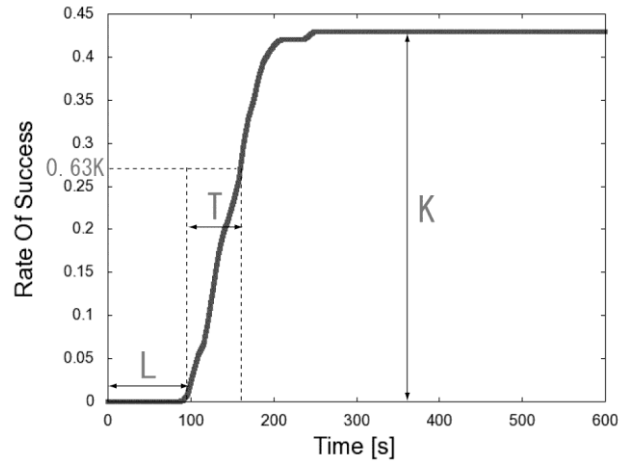

Fig. 10. Parameters used in evaluating the odor source localization cost. This figure shows an example of relationships between the odor source localization success rate and the time required. The success rate increases over time. K is the rate of success. L is the minimum localization time. T is the variance of the localization time, and is determined by K and L.
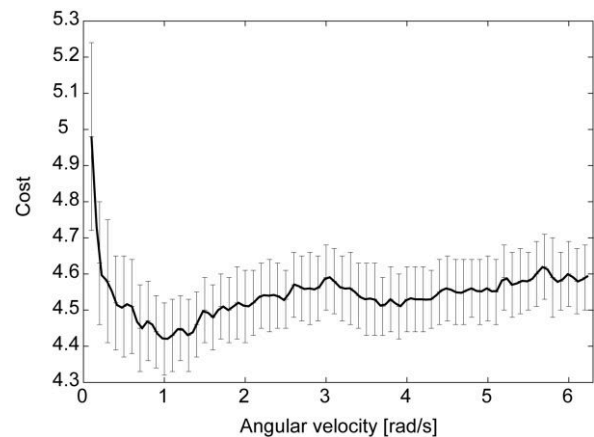

Fig. 11. Evaluation of odor source localization cost. Cost calculated in (3) according to angular velocity from 0.1 rad/s to 6.3 rad/s in increments of 0.1 rad/s are averaged with standard deviations.

By calculating the costs of odor source localization corresponding to each angular velocity from 0.1 rad/s to 6.3 rad/s in increments of 0.1 rad/s, the cost reached a minimum at around 1.0 rad/s (Fig. 11). This means that an angular velocity of around 1.0 rad/s improves the CPT performance. The average angular velocity of real moths is close to 1.0 rad/s. As we discussed above, simply increasing the angular velocity is not the optimum way to reduce the cost, and there is a need for a trade-off between the success rate and the localization time. The angular velocity of a moth should be adapted to an appropriate value through evolution, and a moth maintains its angular velocity using an adaptive sensory feedback system.

It is reported that moths use optomotor responses (feedback responses to maintain the body position using optical cues) during odor source localization [26], [27], [28], [29], [30]. The results of our simulation experiments suggest that a moth maintains its body position during odor source localization.

VII. CONCLUSION

In this study, we showed that an insect could compensate for steering disturbances by controlling its angular velocity, and it had an appropriate behavioral value to minimize the cost in odor source localization. CPT performances given by the appropriate behavioral values suggested in this study can be verified using artificial gas sensors implemented on a mobile robot in real odor environments.

REFERENCES

[1] J. Murlis, C. D. Jones, "Fine-scale structure of odour plumes in relation to insect orientation to distant pheromone and other attractant sources," *Physiol. Entomol.*, vol. 6, no. 1, pp. 71–86, Mar. 1981.

[2] J. Murlis, J. S. Elkinton, R. T. Carde, "Odor plumes and how insects use them," *Annu. Rev. Entomol.*, vol. 37, pp. 505–532, Jan. 1992.

[3] G. Kowaldlo, R. A. Russell, "Robot odor localization: A taxonomy and survey," *Int. J. Robot. Res.*, vol. 27, no. 8, pp. 869–894, Aug. 2008.

[4] J. S. Kennedy, D. Marsh, "Pheromone-regulated anemotaxis in flying moths," *Science*, vol. 184, pp. 999–1001, May. 1974.

[5] D. Marsh, J. S. Kennedy A. R. Ludlow, "An analysis of anemotactic zigzagging flight in male moths stimulated by pheromone," *Physiol. Entomol.* vol. 3, no. 3, pp. 221–240, Sep. 1978.

[6] A. Mafla-Neto, R. T. Carde, "Fine-scale structure of pheromone plumes modulates upwind orientation of flying moths," *Nature*, vol. 369, pp. 142–144, May. 1994.

[7] R. T. Carde, M. A. Willis, "Navigational strategies used by insects to find distant, wind-borne sources of odor," *J. Chem. Ecol.*, vol. 34, no. 7, pp. 854–866, Jul. 2008.

[8] L. P. S. Kuenen, R. T. Carde, "Strategies for recontacting a lost pheromone plume: casting and upwind flight in the male gypsy moth," *Physiol. Entomol.*, vol. 19, no. 1, pp. 15–29, Mar. 1994.

[9] N. J. Vickers, T. A. Christensen, T. C. Baker, "Odour-plume dynamics influence the brain's olfactory code," *Nature*, vol. 410, pp. 466–470, Mar. 2001.

[10] N. Ando, S. Emoto, R. Kanzaki, "Odour-tracking capability of a silkmoth driving a mobile robot with turning bias and time delay," *Bioinspir. Biomim.* vol. 8, no. 1, pp. 1–14, Feb. 2013.

[11] R. Minegishi, A. Takashima, D. Kurabayashi, R. Kanzaki, "Construction of a brain-machine hybrid system to evaluate adaptability of an insect," *Robot. Auton. Syst*, vol. 60, no. 5, pp. 692–699, May. 2012.

[12] R. Minegishi, "Neuroethological study on making adaptive behavior of an insect using a brain-machine hybrid system," Ph.D. dissertation, Dept. Adv. Interdiscip. Stud., The Univ. of Tokyo, Tokyo, Japan, 2012.

[13] E. Kramer, "Orientation of the male silkmoth to the sex attractant bombykol (Book style with paper title and editor)," in *Mechanisms in insect olfaction*, D. A. Denton, J. Coghlan, Ed. New York: Academic Press, 1975, pp. 329–335.

[14] E. Kramer, "Turbulent diffusion and pheromone triggered anemotaxis (Book style with paper title and editor)," in *Mechanisms in insect olfaction*, T. L. Payne, M. C. Birch, C. E. J. Kennedy Ed. Oxford: Clarendon Press, 1986, pp. 59–67.

[15] Y. Obara, "*Bombyx mori* mating dance: an essential in locating the female," *Appl. Entomol. Zool.*, vol. 14, no. 1, pp. 130–132, Feb. 1979.

[16] R. Kanzaki, N. Sugi, T. Shibuya, "Self-generated zigzag turning of *Bombyx mori* males during pheromone-mediated upwind walking," *Zool. Sci.*, vol. 9, no. 3, pp. 515-527, Jun. 1992.

[17] T. Mishima, R. Kanzaki, "Coordination of flipflopping neural signals and head turning during pheromone-mediated walking in a male silkworm moth *Bombyx mori*," *J. Comp. Physiol. A*, vol. 183, no. 3, pp. 273–282, Sep. 1998.

[18] R. Kanzaki, T. Mishima, "Pheromone-triggered 'flipflopping' neural signals correlate with activities of neck motor neurons of a male moth, *Bombyx mori*," *Zool. Sci.*, vol. 13 no. 1, pp. 79–87, Feb. 1996.

[19] C. T. David, "Optomotor control of speed and height by free-flying *Drosophila*," *J. Exp. Biol.*, vol. 82, pp. 389–392, Oct. 1979.

[20] M. V. Srinivasan, "Insect as Gibsonian animals," *Ecol. Psychol.*, vol. 10, no. 3–4, pp. 251– 270, 1998

[21] M. V. Srinivasan, M. Poteser, K. Kral, "Motion detection in insect orientation and navigation," *Vision Res.*, vol. 39, no. 16, pp. 2749–2766, Aug. 1999.

[22] R. Kern, M. Egelhaaf, "Optomotor course control in flies with largely asymmetric visual input," *J. Comp. Physiol. A*, vol. 186, no. 1, pp. 45–55, Jan. 2000.

[23] M. V. Srinivasan, S. Zhang, "Visual motor computations in insects," *Annu. Rev. Neurosci.*, vol. 27, pp. 679–696, Jul. 2004.

[24] T. Takasaki, S. Namiki, R. Kanzaki, "Use of bilateral information to determine the walking direction during orientation to a pheromone source in the silkmoth *Bombyx mori*," *J. Comp. Physiol. A*, vol. 198, no. 4, pp. 295–307, Apr. 2012.

[25] M. Vergassola, E. Villermaux, B. I. Shraiman, "'Infotaxis' as a strategy for searching without gradients," *Nature*, vol. 445, pp. 406–409, Jan. 2007

[26] L. P. S. Kuenen, T. C. Baker, "Optomotor regulation of ground velocity in moths during flight to sex pheromone at different heights," *Physiol. Entomol.*, vol. 7, no. 2, pp. 193–202, Jun. 1982.

[27] H. Y. Fadamiro, T. D. Wyatt, M. C. Birch, "Flying beetle respond as moths predict: Optomotor anemotaxis to pheromone plumes at different heights," *J. Ins. Behav.*, vol. 11, no. 4, pp. 549–557, Jul. 1998.

[28] T. C. Baker, M. A. Willis, P. L. Phelan, "Optomotor anemotaxis polarizes self-steered zigzagging in flying moths," *Physiol. Entomol.* Vol. 9, no. 4, pp. 365–376, Dec. 1984.

[29] N. J. Vickers, T. C. Baker, "Visual feedback in the control of pheromone-mediated flight of *Heliothis virescens* Males (Lepidoptera: Noctuidae)," *J. Insect Behav.*, vol. 7, no. 5, pp. 605–632, Sept. 1994.

[30] R. Vespui, J. R. Gray, "Visual stimuli induced by self-motion and object motion modify odour-guided flight of male moths *(Manduca sexta* L.)," *J. Exp. Biol.*, vol. 212, pp. 3272–3282, Oct. 2009.